Journal of Computer-Aided Molecular Design, **14:** 39–51, 2000.
KLUWER/ESCOM

A molecular-field-based similarity study of non-nucleoside HIV-1 reverse transcriptase inhibitors. 2. The relationship between alignment solutions obtained from conformationally rigid and flexible matching

Jordi Mestres*, Douglas C. Rohrer** & Gerald M. Maggiora
Computer-Aided Drug Discovery, Pharmacia & Upjohn Inc., Kalamazoo, MI 49001, U.S.A.

Received 19 January 1999; Accepted 28 April 1999

Key words: flexible-conformations, molecular alignments, molecular-field similarity, non-nucleoside HIV-1 reverse transcriptase inhibitors

Summary

An analysis of the relationship among alignment solutions obtained from field-based matching of a representative set of rigid conformers of three non-nucleoside HIV-1 reverse transcriptase inhibitors and solutions obtained from flexible matching of the same conformers is presented. In some cases, different alignment solutions obtained from rigid matching converge to the same solution when conformational rigidity is relaxed, indicating that a reduced set of conformers per molecule may be sufficient in many field-based similarity studies. Furthermore, the results also indicate the importance of going beyond the pairwise similarity level to obtain consistent solutions in flexible-matching studies. In this respect, the best conformationally flexible multi-molecule alignment obtained is found to be in good agreement with the relative binding geometry and orientation found experimentally from protein-ligand crystal structures. The rms separation between corresponding atoms in computed and 'experimental' sets of three inhibitor structures is 0.94 Å.

Introduction

Molecular similarity is one of the most widely used concepts in computer-aided approaches to molecular design [1–3]. From database mining [4–7] to pharmacophore identification [8–13] a variety of techniques for assessing the degree of similarity between molecules is routinely being employed. However, both the quantitative measure of the similarity and the computational cost required for its evaluation strongly depend on the way molecular features are represented, which is why simple molecular representations are typically used when searching large compound databases. In contrast, three-dimensional representations of molecules such as steric features (volume and shape), electrostatic and lipophilic potentials, and hydrogen-bond patterns, which are quite complex, may be considered when analyzing the similarity of smaller sets of compounds. Furthermore, these more detailed approaches may be used for assessing the optimal alignment among molecules and, thus, they are well suited for constructing models of relative ligand-binding alignments [14].

As molecules can be superimposed in many different ways, similarity-based molecular-alignment procedures produce a family of superposition solutions which can be ranked using any one of a number of similarity indices [15–18] as a scoring function. One of the main challenges confronting 3D similarity-based methods [19–29] is identification of the 'experimental' alignment amongst the highest ranked alignment solutions, where 'experimental' alignment refers to the relative binding orientation of molecules as would be found by comparison of protein-inhibitor complexes. Here, the 'experimental' relative orientations are extracted from comparisons of the crystal structures of protein-inhibitor bound complexes. The

* Present address: Department of Molecular Design & Informatics, N.V. Organon, P.O. Box 20, 5340 BH Oss, The Netherlands.
**To whom correspondence should be addressed.

protein-inhibitor crystal structures also provide valuable information about the preferred conformation of the bound molecules (the bioactive conformation). Using the molecular structures of inhibitors in their enzyme-bound conformation, it has recently been shown that 3D molecular-field-based similarity analyses are able to rank the 'experimental' alignment as the best molecular-field alignment solution [30, 31].

At the initial stages of the drug-design process, crystal structures of protein-inhibitor complexes are unlikely to be available. Consequently, information about the bioactive conformation of effector molecules must be gained indirectly. In these cases, the number of conformational isomers for each molecule further complicates identification of the 'experimental' alignment. In this respect, treatment of conformational flexibility inherent in 3D molecular structures is essential if high quality molecular alignments are to be obtained [33, 34]. One of the pioneering molecular-alignment strategies accounting for conformational flexibility is the active-analog approach [34]. This is a feature-based strategy which explores accessible conformations in a series of molecules looking for positional commonality between selected features and the location of previously selected pharmacophoric groups.

More recently, some atom-based strategies [35] have also proved efficacious in superposing sets of flexible molecules, and a number of shape-based [23, 24] and field-based [26–29] methods that include some level of conformational flexibility have been developed and applied to a variety of problems in drug design. However, despite the significance of atom-based and feature-based methods in producing reasonable alignments at a relatively low computational cost, they require explicit specification of atoms or features within each molecule. The resulting alignments tend either to be too directly associated with the spatial position of individual atoms or require a feature-by-feature correspondence to the pharmacophoric mapping. In contrast, shape-based and field-based alignment methods are less dependent on specific atomic positions of selected atoms or groups and, thus, they appear to be better qualified for obtaining less biased molecular alignments. The size of the problem (in terms of number of molecules and their flexibility) and the amount and type of experimental structural information available (which may provide some clues on a preferred alignment) will finally determine the ultimate choice of a particular similarity-based method.

The main aim of the present work is to analyze the scope and limitations of allowing conformational flexibility during field-based similarity studies. For this purpose, alignment solutions obtained from rigid and flexible matching will be compared and analyzed in detail. An illustrative example is presented based on a set of three non-nucleoside HIV-1 reverse transcriptase inhibitors (NNRTIs), possessing different degrees of conformational flexibility [31].

Methodological aspects

Molecular structure analysis

The first step in any molecular comparison approach must be a consideration of the molecular structures themselves. The procedure outlined in Scheme 1 describes the approach employed in obtaining a set of conformations for each molecule which was used in the similarity comparisons. In this study, a preliminary structure for each of the molecules was generated using molecular modelling and structure refinement techniques employing an MM2* molecular mechanics potential-energy minimization approach [36]. Solvent effects were included through the GB/SA model as implemented in the MOSAIC program [37]. Since there is no assurance that a molecule will bind in its lowest-energy conformation, the conformational space of each molecule was explored by systematically varying the torsional angles in rotatable bonds and flexible rings using a pseudo Monte Carlo search [38], followed by energy minimization retaining those conformations within 5 kcal/mol of the minimum. The sets of conformations thus generated for each molecule were then examined using a principle-components analysis of the pairwise conformational similarity matrix derived from the sets conformations (N.B. only the steric-field similarity formula described below was used to evaluate the similarities). Clustering of the conformations was accomplished by consideration of the three largest components. The lowest energy conformation from each cluster was selected as a representative subset of conformations within each cluster. This yields a reduced set of prototype conformations that 'cover' the conformational space of each molecule.

Molecular similarity

All molecular-field-based similarity calculations were performed with the program MIMIC [29]. Two 3D

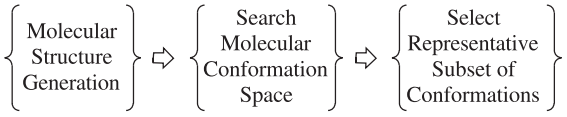

Scheme 1. The molecular structure modelling approach.

scalar molecular fields are evaluated for each molecule, a single-Gaussian atom-centered field to represent the steric features [39] and an atomic point-charge electrostatic potential to represent the electrostatic features of a molecule [40]. The 1/r term in the latter is approximated by a sum of three Gaussian functions to avoid divergences at atomic positions [41]. Although these approximations may be considered to be rather crude, they are generally sufficient to account for the essential steric and electrostatic characteristics of most molecules. Moreover, they lead to significant speed ups in the field-based similarity calculations.

Once a given molecular field (MF) has been defined, a field-based similarity measure between two molecules A and B (Z_{AB}^{MF}) is defined as [15]:

$$Z_{AB}^{\mathrm{MF}} = \int F_A^{\mathrm{MF}}(\mathbf{r}) F_B^{\mathrm{MF}}(\mathbf{r}) d\mathbf{r}, \tag{1}$$

where $F_A^{\mathrm{MF}}(\mathbf{r})$ and $F_B^{\mathrm{MF}}(\mathbf{r})$ are the MFs of molecules A and B, respectively. If A and B are the same molecule, the value obtained from Equation 1 is then a measure of the molecular self-similarity (Z_{AA}^{MF} and Z_{BB}^{MF} for molecules A and B, respectively). However, in order to compare similarity values from different pairs of molecules, similarity measures are usually normalized to obtain a similarity index. Throughout this work, the similarity index between two molecules A and B (S_{AB}^{MF}) is given by [15]:

$$S_{AB}^{\mathrm{MF}} = \frac{Z_{AB}^{\mathrm{MF}}}{(Z_{AA}^{\mathrm{MF}} \cdot Z_{BB}^{\mathrm{MF}})^{1/2}}. \tag{2}$$

The range of possible values of S_{AB}^{MF} lies in the unit interval $[0, +1]$ for positive-definite molecular steric volume (MSV) fields and within $[-1, +1]$ for non-positive-definite molecular electrostatic potential (MEP) fields. Ultimately, a combined similarity index, S_{AB}, encompassing the two MFs may be defined as a weighted combination of the similarities:

$$S_{AB} = \lambda S_{AB}^{\mathrm{MSV}} + (1 - \lambda) S_{AB}^{\mathrm{MEP}}. \tag{3}$$

Based on previous validation studies [29–31], a combined similarity index containing a 2:1 relationship between the steric-field, $\lambda = 0.667$, and the electrostatic-field, $(1 - \lambda) = 0.333$, similarities was employed. In all cases, the similarity between the molecules was fully maximized by varying the relative orientation and position between molecules. (A similarity calculation was considered optimized when the gradient norm of the similarity index was below 10^{-4}.)

Details on the molecular-field approximations and the similarity calculations as implemented in MIMIC can be extensively found elsewhere [29–31].

Conformationally rigid similarity analysis

As indicated in Scheme 2, analysis of the conformational flexibility of molecules in field-based similarity matching is carried out in several stages. The first stage involves comparisons of the representative 'prototype' structures contained in the conformational subsets for each molecule obtained during structure modelling. These structures characterize the intrinsic flexibility of the individual molecules. A systematic evaluation of the similarities between all possible pairs of representative conformers of the different molecules was performed. At this level, optimization of S_{AB} depends only on the three translational ($\mathbf{t}$) and the three rotational ($\boldsymbol{\theta}$) degrees of freedom. The different conformers are treated as internally rigid, Z_{AA}^{MF} and Z_{BB}^{MF} therefore remain constant during the optimization and, thus, $S_{AB}^{\mathrm{MF}}(\mathbf{t}, \boldsymbol{\theta})$ in Equation 4 is only a function of $Z_{AB}^{\mathrm{MF}}(\mathbf{t}, \boldsymbol{\theta})$. For this reason, the similarity matching of the different conformations will be referred to as a conformationally rigid matching.

$$S_{AB}^{\mathrm{MF}}(\mathbf{t}, \boldsymbol{\theta}) = \frac{Z_{AB}^{\mathrm{MF}}(\mathbf{t}, \boldsymbol{\theta})}{(Z_{AA}^{\mathrm{MF}} \cdot Z_{BB}^{\mathrm{MF}})^{1/2}} \tag{4}$$

Conformationally flexible similarity analysis

At the second stage, flexible torsional angles in each representative conformer of one molecule, the adapting molecule, are included as degrees of freedom during the similarity matching procedure. Starting from the matches obtained during the conformationally rigid stage, the similarity between the molecules

Scheme 2. Similarity matching approach.

is then optimized by varying all translational (**t**), rotational (**θ**), and torsional (**τ**) components. For this reason, a flexible similarity matching at this level will be referred to as a conformationally flexible matching.

$$S_{AB}^{\mathrm{MF}}(\mathbf{t}, \boldsymbol{\theta}, \boldsymbol{\tau}) = \frac{Z_{AB}^{\mathrm{MF}}(\mathbf{t}, \boldsymbol{\theta}, \boldsymbol{\tau})}{(Z_{AA}^{\mathrm{MF}} \cdot Z_{BB}^{\mathrm{MF}}(\boldsymbol{\tau}))^{1/2}} \tag{5}$$

Note that, although no energy constraint is explicitly introduced to restrict the range of conformational flexibility in molecules, the use of similarity indices directly prevents the formation of undesirable intra-molecular steric clashes. Since the conformation changes during conformationally flexible matching, the value of in Equation 5 depends on both (as is the case for conformationally rigid matching) and also on the changing value of the self-similarity value. If steric clashes begin to appear in the molecule, its self-similarity (its internal steric overlap, see Equation 1) will increase in value. As a consequence, the maximization of *SAB* becomes a balance between increasing the inter-molecular overlap while avoiding too close intra-molecular steric contacts.

Multi-molecule similarity matching

Multi-molecule similarity alignments were obtained from the conformationally flexible pairwise matching results by simultaneously considering entire sets of M molecules. A similarity index quantifying the similarity of each set of more than two molecules is evaluated by averaging all possible pairwise similarities in the set. Thus, for a set of M molecules, $M \cdot (M-1)/2$ pairwise similarities have to be computed and the multi-molecule similarity, S_M, is then estimated as in Equation 6.

$$S_M = \left[\frac{M \cdot (M-1)}{2}\right]^{-1} \sum_{I<J} S_{IJ} \tag{6}$$

Multi-molecule alignments are initially constructed by directly superimposing the relative orientations of $(M-1)$ molecules to a given reference molecule, according to the different alignment solutions obtained from the explorations of the conformationally flexible pairwise similarity matching. Then, each multi-molecule alignment is optimized to maximize S_M as given in Equation 6. Since the relative orientation of all molecules is optimized, multi-molecule alignment solutions should not be dependent on the molecule selected as reference [31].

Results and discussion

Three NNRTIs, namely, Nevirapine (NEVI) [42], the TIBO R86183 analog (TIBO) [43], and the αAPA R95845 analog (αAPA) [44], have been selected to illustrate the performance of the present flexible-matching approaches in assessing the 'experimental' alignment of molecules. The molecular structures of these inhibitors are depicted in Scheme 3. This set of inhibitors was selected because it was used recently [31] as a basis for analyzing the ability of molecular-field-based similarity methods to reproduce the 'experimental' alignment obtained for these three inhibitors from a comparison of the crystal structures of their respective HIV-1 RT/inhibitor complexes. In the following sections, a systematic procedure for obtaining multi-molecule alignments from conformationally flexible matching is presented. This includes conformational analysis and clustering to select a set of representative conformers for each molecule, exploration of the pairwise similarity spaces between representative conformers of the molecules, and construction of multi-molecule alignments from the pairwise-alignment solutions.

Conformational analysis and clustering

As is evident from Scheme 3, NEVI has two torsional angles in the seven-member ring and one exo-cyclic torsional angle to the cyclopropyl, TIBO has three torsional angles in the seven-member ring and two exo-cyclic torsional angles in the 3-methyl-3-butene side chain, and αAPA has five acyclic torsional angles to be explored. Within a range of 5 kcal/mol from the lowest-energy conformer located for each molecule, the conformational analyses gave rise to 2, 20, and 37 unique energy-minimized conformers for NEVI, TIBO, and αAPA, respectively. Consideration of all these conformers in the subsequent conformationally rigid similarity analysis would result in exploring 40 {NEVI,TIBO}, 74 {NEVI,αAPA}, and 740 {TIBO,αAPA} pairwise conformational combinations and, consequently, 1480 {NEVI,TIBO,αAPA} three-molecule conformational combinations. A similarity analysis of this magnitude becomes fairly tedious, at best. One cycle of pairwise similarity comparison of 40 atom structures using the MIMIC program on a Silicon Graphics Octane computer with a 250 MHz R10000 MIPS processor requires approximately 0.02 seconds of CPU time. Since a typical rigid similarity maximization requires on the order of 10 to 20

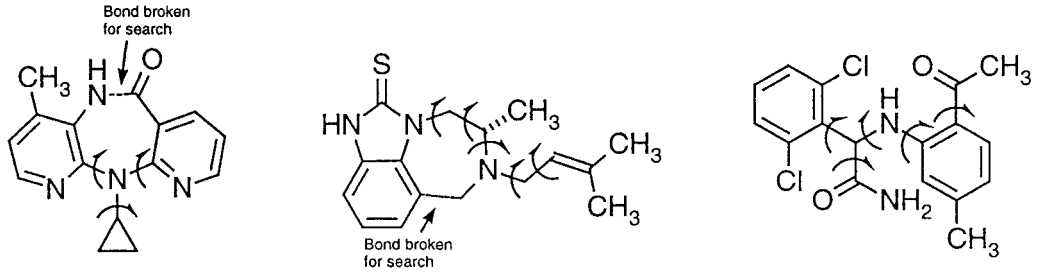

Nevirapine TIBO R86183 αAPA R95845

Scheme 3. NNRTIs: Curved arrows represent the torsional degrees-of-freedom considered.

cycles to converge to a gradient less than 0.001, 0.3 to 0.6 s/pair may be required for each rigid match. Pairwise flexible matching would require from 25 to 200 additional cycles to converge depending on the number of bonds allowed to rotate. Therefore, a full pairwise rigid/flexible-conformation similarity maximization may require from 0.7 to 4.5 seconds or more for each pairwise match. Alternative optimization parameters and/or structural considerations could easily reduce these compute times by a factor of 10, if necessary, with a corresponding reduction in precision and accuracy. While the computer time required is not prohibitive, the volume of data generated can easily become overwhelming. Therefore, early reduction of the number of conformations considered makes the analysis much easier.

A strategy that can be used to reduce the complexity of the similarity analysis is to look for structural commonalties among conformers in an attempt to identify groups of similar conformers within localized regions of conformational space. A representative conformation can then be selected from each localized region, thus reducing the number of conformations which must be considered. This is usually referred to as conformational clustering. In MIMIC, this is done by constructing the pairwise steric-field similarity matrix between all conformers of a given molecule and then clustering the similarity matrix by means of a principal component analysis. After performing the conformational clustering, the lowest-energy conformer in each cluster is selected as a representative conformer of the set of conformers within the cluster [29]. Besides the two conformers found for NEVI in the initial search, the above procedure yielded three representative conformers for both TIBO and αAPA. The numbers shown in parentheses following the inhibitor name identify the relative energy ranking of the conformations selected. Accordingly, the complexity of the similarity analysis is significantly reduced to the exploration of 6 {NEVI,TIBO}, 6 {NEVI,αAPA}, and 9 {TIBO,αAPA} pairwise similarity combinations and 18 {NEVI,TIBO,αAPA} three-molecule similarity spaces, a much more manageable computational task. To gain a visual sense of the conformational diversity covered by the representative conformers, their superposed structures are depicted in Figure 1.

The energy differences and the overall rank in energy of the representative conformers with respect to the lowest-energy conformer for each molecule are collected in Table 1. As expected, the two representative mirror-image conformers of NEVI are degenerate in energy. Interestingly, the three representative conformers selected for TIBO and αAPA do not correspond to the three lowest-energy conformers, but span a wide energy range. Especially remarkable is the case of TIBO(3), which has an energy 3.60 kcal/mol above the lowest energy conformer, TIBO(1), and ranked fourteenth in energy out of 20 TIBO conformers.

Also included in Table 1 are the steric- and electrostatic-field similarities between each representative conformer and the corresponding structure of the inhibitor in its bound form as observed crystallographically. The crystal structures of the NEVI, TIBO, and αAPA molecules were extracted from the Protein Data Bank (PDB) [45] with codes 3HVT [46], 1HNV [47], and 1HNI [48], respectively. The values of both the steric- and electrostatic-field similarity indices indicate that among the different representative conformers, NEVI(1) and TIBO(1) are clearly the most similar conformers to the NEVI and TIBO protein-bound conformations. This is substantiated by the small values, less than 1 Å, of the rms distances between the corresponding atoms of the conformer structures and the crystal structures. In contrast, while

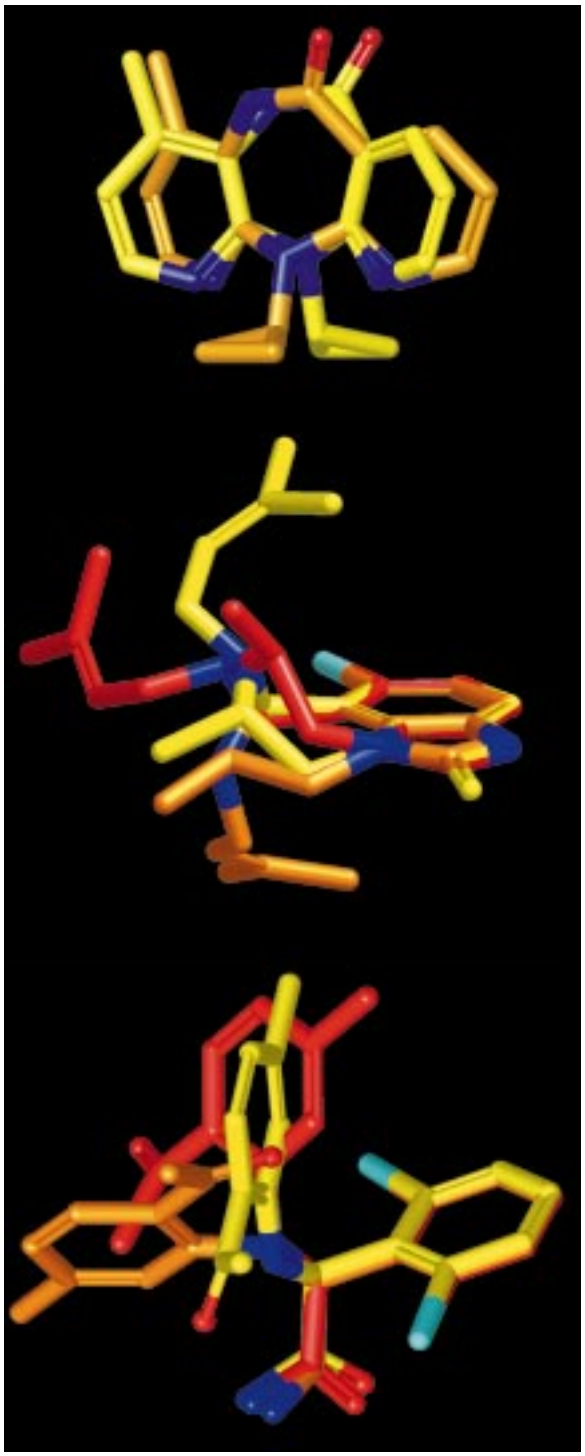

Figure 1. Selected representative conformations for NEVI (top), TIBO (middle), and αAPA (bottom). The lowest energy conformations are colored in yellow (referred to as NEVI(1), TIBO(1), and αAPA(1) in the text) and higher-energy conformations are given in orange (referred to as NEVI(2), TIBO(2), and αAPA(2) in the text) and red (referred to as TIBO(3) and αAPA(3) in the text), in increasing order of energy.

Table 1. Potential energy and structure comparison data[a] for representative conformers for each NNRTI molecule

Conformer[b]	ΔE (Rank)[c]	S^{MSV}	S^{MEP}	Rms[d]
NEVI(1)	0.00 (1)	0.9146	0.9510	0.35
NEVI(2)	0.00 (1)	0.8273	0.8280	4.27
TIBO(1)	0.00 (1)	0.9066	0.9544	0.93
TIBO(2)	1.05 (3)	0.7714	0.7824	2.08
TIBO(3)	3.60 (14)	0.7824	0.7498	1.52
αAPA(1)	0.00 (1)	0.8240	0.8337	2.06
αAPA(2)	1.05 (5)	0.8306	0.7292	1.52
αAPA(3)	1.47 (9)	0.8191	0.6891	3.90

[a]For each inhibitor, S^{MSV} and S^{MEP} are, respectively, the steric- and electrostatic-field similarity indices between the corresponding crystal structure and each representative conformer.
[b]The number shown in parentheses refers to the relative energy ranking of the representative conformers for each inhibitor.
[c]Energy difference (ΔE) is given in kcal/mol. Also given in parentheses is the rank in energy among all the conformers with respect to the lowest-energy conformer located for each molecule.
[d]The root-mean-square (rms) values are the separations (in Å) between corresponding non-hydrogen atoms of the representative conformers and the crystal structure.

the steric-field similarity indices and rms distance comparisons indicate that αAPA(2) has the structure closest to that of the αAPA protein-bound conformation, its electrostatic-field similarity index is lower than that of αAPA(1). At this point, however, identification of the closest structural representative among the starting subset is all that is required. Therefore, NEVI(1), TIBO(1) and αAPA(2) will be considered the structures representative of the 'experimental' conformations. It is also worth remarking that the values of the similarity indices found for the representative conformers of αAPA are smaller than the values found for NEVI(1) and TIBO(1). This indicates that the conformational analysis of αAPA did not provide as good a characterization of the protein-bound structure of αAPA as was obtained for NEVI and TIBO. All these aspects influence the results of the similarity analysis and test the scope and limitations of the flexible matching approach.

Exploration of the pairwise similarity spaces

An exhaustive exploration of the similarity spaces induced by each molecular pair was performed to locate the different pairwise alignment solutions, i.e., the set of relative orientations that maximize the similarity between each pair of molecules. Since each molecule

is actually represented by a number of conformers, pairwise similarity spaces between all combinations of representative conformers of the respective molecules have to be explored. The systematic spherical-search algorithm implemented in MIMIC was used to perform the similarity-space explorations [29]. This procedure requires that one structure be kept fixed (the reference structure) while the other (the adapting structure) is systematically placed in a series of unique starting orientations about the reference structure. The similarity between two molecular structures is then optimized using a common gradient-seeking procedure, which ensures that a wide and uniformly distributed exploration of the similarity between the molecular-field representations of the two molecular structures is obtained. Once such a conformationally rigid alignment solution has been obtained, the appropriate rotatable bonds of the adapting molecule are allowed to undergo torsional movement. The similarity between the two structures is then optimized with respect to all translational, rotational, and torsional degrees-of-freedom yielding a conformationally flexible match.

The five best similarity results obtained from exploration of all pairwise combinations of {NEVI, TIBO} and {NEVI,αAPA} representative conformers are presented in Tables 2 and 3, respectively. These similarity indices are given for both the conformationally rigid and the conformationally flexible matching. Those alignments in closest agreement with the 'experimental' alignment are marked in bold.

The fifth-best alignment solution (0.6058) obtained from the exploration of the {NEVI(1),TIBO(1)} similarity space is in good qualitative agreement with the 'experimental' alignment, at the conformationally rigid level, see Table 2. This alignment solution is ranked 28th among all {NEVI,TIBO} alignment solutions. Subsequent optimization at the conformationally flexible level improves its similarity ranking (0.6740) to ninth-best overall, and second within the {NEVI(1),TIBO(1)} set.

Two conformationally rigid pairwise matches for {NEVI,αAPA}, the fifth (0.5493) for {NEVI(1),αAPA (2)} and second (0.5487) for {NEVI(1),αAPA(1)}, are in qualitative agreement with the 'experimental' alignment, see Table 3. Overall, their similarity indices are ranked 14th and 15th respectively. Refinement of these alignments at the conformationally flexible level moves their placement to 16th (0.6292) and 20th (0.6262) place among the {NEVI,αAPA} conformationally flexible alignment solutions.

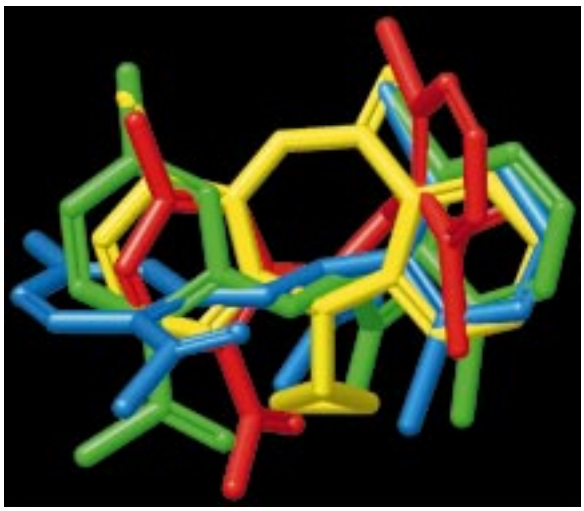

Figure 2. Convergence of conformationally rigid alignment solutions from two different conformations to the same flexible alignment solution. The structure of the NEVI reference conformer, NEVI(1), is given in yellow, the rigid alignment solutions of two αAPA conformers, αAPA(1) and αAPA(2), are given in red and blue respectively, and the flexible alignment solution achieved independently from each one of the previous rigid alignment solutions is given in green.

The calculated atomic charges for each structure are different for each conformation. Since the atomic charges are held fixed during the conformationally flexible alignment, differences in the similarity indices in Table 3 resulting from differences in the atomic charges may obscure situations where the structures may have converged to the same conformation. This situation is illustrated in Figure 2. Taking NEVI(1) (yellow structure) as the reference structure, the relative orientations of αAPA(1) (in red) and αAPA(2) (in blue) correspond to the second (0.5487) and fifth (0.5493) conformationally rigid matches respectively. This is an example where comparable values of similarity indices are associated with different molecular alignments. As can be observed, while the match involving αAPA(1) aligns the 2-acetyl-5-methylphenyl ring to the 4-methyl-pyridine ring of NEVI(1) leaving the dibromophenyl ring to project above the NEVI(1) structure, the αAPA(2) match overlaps the dibromophenyl ring upon the NEVI(1) pyridine ring which places the 2-acetyl-5-methylphenyl ring nearly perpendicular to the NEVI(1) structure. However, when these two conformationally rigid alignments are further optimized at the conformationally flexible level (the five rotatable αAPA bond-torsional angles are included as degrees of freedom to maximize the similarity), they converge to the same alignment solution

Table 2. Similarity indices corresponding to the five best molecular overlays obtained from the exploration of the similarity space induced by the {NEVI,TIBO} pair

Conformational pair	Similarity indices for conformationally rigid matching[a]				
	1	2	3	4	5
{NEVI(1),TIBO(1)}	0.6795	0.6354	0.6261	0.6249	**0.6058**
{NEVI(1),TIBO(2)}	0.6642	0.6641	0.6486	0.6332	0.6330
{NEVI(1),TIBO(3)}	0.6544	0.6275	0.6237	0.6128	0.5975
{NEVI(2),TIBO(1)}	0.6815	0.6667	0.6249	0.6199	0.6197
{NEVI(2),TIBO(2)}	0.6672	0.6400	0.6297	0.6251	0.6244
{NEVI(2),TIBO(3)}	0.6549	0.6174	0.6137	0.6128	0.5982
Conformational pair	Similarity indices for conformationally flexible matching[a,b]				
	1′	2′	3′	4′	5′
{NEVI(1)|TIBO(1)}	0.6956(1)	**0.6740(5)**	0.6436(2)	0.6377(7)	0.6355(4)
{NEVI(1)|TIBO(2)}	0.6913(3)	0.6872(1)	0.6547(4)	0.6176(6)	0.6144(7)
{NEVI(1)|TIBO(3)}	0.6995(1)	0.6738(2)	0.6363(9)	0.6291(17)	0.6140(5)
{NEVI(2)|TIBO(1)}	0.6845(2)	0.6840(30)	0.6834(1)	0.6418(3)	0.6417(24)
{NEVI(2)|TIBO(2)}	0.6808(1)	0.6659(2)	0.6547(6)	0.6345(3)	0.6297(4)
{NEVI(2)|TIBO(3)}	0.6600(7)	0.6561(1)	0.6437(6)	0.6390(3)	0.6364(2)

[a]The bolded similarity index corresponds to the alignment closest to the 'experimental' alignment.
[b]The number in parentheses refers to the conformationally rigid matching overlay from which the conformationally flexible match originated.

Table 3. Similarity indices corresponding to the five best molecular overlays obtained from the exploration of the similarity space induced by the {NEVI,αAPA} pair

Conformational pair	Similarity indices from conformationally rigid matching[a]				
	1	2	3	4	5
{NEVI(1),αAPA(1)}	0.5734	**0.5487**	0.5426	0.5396	0.5256
{NEVI(1),αAPA(2)}	0.5679	0.5632	0.5572	0.5504	**0.5493**
{NEVI(1),αAPA(3)}	0.5463	0.5418	0.5231	0.5173	0.5163
{NEVI(2),αAPA(1)}	0.5882	0.5738	0.5575	0.5525	0.5472
{NEVI(2),αAPA(2)}	0.5746	0.5509	0.5449	0.5417	0.5412
{NEVI(2),αAPA(3)}	0.5959	0.5651	0.5405	0.5339	0.5318
Conformational pair	Similarity indices from conformationally flexible matching[a,b]				
	1′	2′	3′	4′	5′
{NEVI(1)|αAPA(1)}	0.6540(5)	0.6387(1)	0.6304(5)	0.6301(3)	**0.6292(2)**
{NEVI(1)|αAPA(2)}	0.6356(2)	0.6311(19)	**0.6262(5)**	0.6220(4)	0.6206(3)
{NEVI(1)|αAPA(3)}	0.6440(13)	0.6328(16)	0.6293(4)	0.6290(1)	0.6277(12)
{NEVI(2)|αAPA(1)}	0.6379(1)	0.6332(17)	0.6197(8)	0.6194(7)	0.6142(2)
{NEVI(2)|αAPA(2)}	0.6547(33)	0.6364(2)	0.6280(9)	0.6260(28)	0.6226(1)
{NEVI(2)|αAPA(3)}	0.6496(5)	0.6311(7)	0.6231(1)	0.6208(51)	0.6114(2)

[a]The bolded similarity index corresponds to the alignment closest to the 'experimental' alignment.
[b]The number in parentheses refers to the conformationally rigid matching overlay from which the conformationally flexible match originated.

(in green). These results reveal two important points. First, structurally equivalent alignments which result from convergence to a common solution from diversified initial conformations may produce different combined similarity indices because of differences in the starting structural geometries and atomic charge

sets which remain fixed. Second, it may not be necessary to consider every energy-minimized conformer in molecular-field-based similarity studies when conformational flexibility is employed. These results show that flexible matching allows 'migration' within conformational space in a way that overcomes conformational deficiencies in the selected structure and indicate that using a reduced number of diverse conformers is equivalent to exploring a large region of conformational space.

Construction of multi-molecule alignments

Earlier studies [30, 31] and the results above strongly suggest that extension beyond pairwise similarity may be required to obtain high-ranking alignment solutions in agreement with the 'experimental' alignment. In the same studies, the highest ranking multi-molecule similarity was found to identify a consensus multi-molecule alignment that agreed with the 'experimental' alignment.

Table 4 collects the six highest-ranked similarity values corresponding to the best three-molecule alignments. These data were obtained from consideration of three-molecule alignment combinations constructed from all the pairwise alignments using either NEVI(1) or NEVI(2) as the reference molecule with each of the three representative conformers of TIBO and each of the three representative conformers of αAPA. As is observed, the best three-molecule alignment solution (labeled as rank I with a similarity index of 0.6533) is obtained by taking NEVI(2) as reference and optimizing the relative orientation of TIBO(1) and αAPA(3). Originally, this three-molecule alignment was constructed by superimposing TIBO(1) and αAPA(3) on NEVI(2) according to the third-best (0.6834) and best (0.6496) conformationally flexible alignments for {NEVI(2),TIBO(1)} and {NEVI(2),αAPA(3)} (see Tables 2 and 3). According to Equation 6, this resulted in an initial three-molecule similarity index of 0.6477, which increased to 0.6533 after optimization.

The three-molecule alignment which is in good agreement with the 'experimental' alignment (marked in bold in Table 4) appears now as the second-best alignment among all three-molecule alignments constructed. This is a significant improvement in comparison with the corresponding similarity ranking obtained at the pairwise level of similarity. Actually, a 'degenerate' solution for this three-molecule alignment is independently obtained in this case, with similarity indices of 0.6501 and 0.6479 (both labeled as rank II). This is a direct consequence of the fact commented on above that the fifth-best alignment in {NEVI(1),αAPA(1)} and the third-best alignment in {NEVI(1),αAPA(2)} were already 'degenerate' alignment solutions at the conformationally flexible level (see Figure 2). Accordingly, the difference of 0.0022 in the values of the two three-molecule similarity indices comes from the structural differences and, consequently, also from differences in the atomic charges of the original energy-minimized αAPA(1) and αAPA(2) conformers. A similar situation is encountered in the best three-molecule alignments found among {NEVI(2),TIBO(1),αAPA(1)} and {NEVI(2),TIBO(1),αAPA(2)} (both labeled as rank III).

Two limitations exist in the present approach to treatment of conformational flexibility in molecular-field-based similarity studies, namely, total geometry relaxation and charge redistribution are not allowed during the flexible matching. In the two- and three-molecule degenerate alignments described above, subtle geometry differences are responsible for the differences in the steric-field similarity, while the charge distribution differences produce the variations in the electrostatic-field similarity. However, as molecular conformations have been mutually adapted to maximize the field-based similarity, the differences in electrostatic-field similarity are clearly more important than the differences in steric-field similarity. In the present work, this can be shown when analyzing the steric- and electrostatic-field contributions to the final combined field-based similarity index. For the 'degenerate' three-molecule alignments in good agreement with the 'experimental' alignment, the steric- and electrostatic-field contributions to the total combined similarity indices were 0.6625 and 0.6252, respectively, for {NEVI(1),TIBO(1),αAPA(1)}, resulting in a combined similarity index of 0.6501. For {NEVI(1),TIBO(1),αAPA(2)} the corresponding indices were 0.6621 and 0.6195, respectively, to give 0.6479. Thus, for this particular case, the differences from the steric- and the electrostatic-field similarities are 0.0004 and 0.0057, respectively, which represent a contribution of 12.3% and 87.7% to the total difference (0.0022) between the two combined similarity indices each based on a (2:1) weighted average of the steric- and electrostatic-field indices.

To quantitatively analyze the dependence of field-based similarities on charge redistribution and to alleviate the similarity index differences resulting from inappropriate differences in the electrostatic-field sim-

Table 4. The five highest three-molecule alignments obtained by optimization of the representative NNRTIs before and after atomic charge re-evaluation

Rank	Molecular set	Pairwise similarity indices from three-molecule matching[a]			
		{NEVI,TIBO}	{NEVI,αAPA}	{TIBO,αAPA}	S_M^b
I	{NEVI(2),TIBO(1),αAPA(3)}	0.6797	0.6481	0.6322	0.6533(3,1)
II	{NEVI(1),TIBO(1),αAPA(1)}	0.6736	0.6284	0.6483	**0.6501(2,5)**
II	{NEVI(1),TIBO(1),αAPA(2)}	0.6735	0.6252	0.6449	**0.6479(2,3)**
III	{NEVI(2),TIBO(1),αAPA(1)}	0.6834	0.6185	0.6315	0.6445(2,4)
III	{NEVI(2),TIBO(1),αAPA(2)}	0.6834	0.6216	0.6264	0.6438(2,5)
IV	{NEVI(1),TIBO(3),αAPA(1)}	0.6724	0.6532	0.6004	0.6420(2,1)
Rank	Molecular set	Pairwise similarity indices from three-molecule matching following re-evaluation of the atomic charges[a]			
		{NEVI,TIBO}	{NEVI,αAPA}	{TIBO,αAPA}	S_M^b
I′	{NEVI(1),TIBO(1),αAPA(2)}	0.6731	0.6241	0.6514	**0.6495(2,3)**
I′	{NEVI(1),TIBO(1),αAPA(1)}	0.6732	0.6228	0.6499	**0.6486(2,5)**
II′	{NEVI(2),TIBO(1),αAPA(2)}	0.6796	0.6224	0.6400	0.6473(2,5)
II′	{NEVI(2),TIBO(1),αAPA(1)}	0.6795	0.6161	0.6447	0.6468(2,4)
III′	{NEVI(2),TIBO(1),αAPA(3)}	0.6801	0.6346	0.6259	0.6468(3,1)
IV′	{NEVI(1),TIBO(3),αAPA(1)}	0.6707	0.6590	0.6095	0.6464(2,1)

[a]The bolded similarity index corresponds to the alignment closest to the 'experimental' alignment.
[b]The numbers in parentheses refer to the conformationally flexible pairwise matches, {NEVI,TIBO} and {NEVI,αAPA} respectively, used to generate the initial three-molecule alignment, see Tables 2 and 3.

ilarities for degenerate conformations, atomic charges were recomputed from each of the final conformationally adapted structures. Then, the three-molecule alignments previously obtained were re-optimized. The results of this analysis are collected in Table 4. Interestingly, the best three-molecule alignment obtained corresponds now to the alignment in closest agreement with the 'experimental' alignment. This actual best three-molecule alignment is a 'degenerate' solution, with similarity indices of 0.6495 and 0.6486, which has been promoted from the second-best solution (rank II) to the best solution (rank I′) after accounting for charge redistribution to evaluate the electrostatic-field similarity contribution to the total combined (2:1) similarity index. This also reduces the remaining difference between the two 'degenerate' alignments from 0.0022 to 0.0009. On the other hand, the best three-molecule alignment solution obtained when atomic charges from minimum-energy structures were being used to evaluate the electrostatic-field similarity (rank I) is now the third-best alignment (rank III′). Thus, although the three best three-molecule alignments have interchanged their relative ordering, they have maintained their privileged position in similarity ranking with respect to the rest of the three-molecule alignments.

It is worth emphasizing the fact that the final best three-molecule alignment corresponds to the solution in closest agreement with 'experiment', which is remarkable given the subtle discrimination between the similarity values of different three-molecule alignment solutions. What is important at this stage is that a consensus three-molecule alignment close to the 'experimental' alignment is found among the top alignment solutions, which represents a significant improvement from the situation encountered at the pairwise similarity level. The poor discrimination between similarity values of the conformationally flexible three-molecule alignment solutions is a direct consequence of the flexible matching. This is also an interesting result which deserves consideration because as structures are allowed to adapt to each other, the differences in similarity between the alignment solutions are significantly reduced.

At this point, it would be interesting to recompute the similarity between the final conformationally adapted structures of TIBO and αAPA, as obtained in the best three-molecule alignments, and their corresponding receptor-bound crystal structures. Comparison of these similarities with those values reported initially in Table 1 when the energy-minimized conformers were considered will permit to assess the use-

fulness of flexible matching to approach the respective experimental conformations. The steric-field similarity between the conformationally adapted TIBO(1) structure and its corresponding crystal structure conformation (as extracted from PDB code 1HNV) is 0.8946, slightly smaller than the steric-field similarity obtained for the original minimum-energy TIBO(1) conformer (0.9066 in Table 1). With respect to the electrostatic-field similarity, similarity indices of 0.9363 and 0.9384 were obtained when using atomic charges from minimum-energy or conformationally adapted structures, respectively. Despite showing a high degree of similarity, after a conformationally flexible matching these values are also smaller than those obtained from the minimum-energy TIBO(1) structure (0.9544 in Table 1). As regards αAPA(2), the steric-field similarity between its conformationally adapted structure and the corresponding crystal structure conformation (as extracted from the PDB code 1HNI) is 0.9202, clearly larger than the value of 0.8306 reported originally in Table 1. On the other hand, the electrostatic-field similarities obtained when using atomic charges from minimum-energy or conformationally adapted structures are, respectively, 0.8433 and 0.8425, also larger than the 0.7292 value in Table 1. Thus, it is found that in the case where a representative conformer has initially a high degree of similarity with respect to its experimental conformation (as in the case of TIBO(1)), the flexible matching returned an adapted conformation not much different from the original one. In contrast, in the case showing a lower degree of similarity in comparison to the experimental conformation (as in the case of αAPA(1) and αAPA(2)), the flexible matching moved toward the αAPA crystal structure conformation. For this particular set of molecules, the use of flexible matching appears as a reasonable strategy to obtain good conformations of molecules.

After accounting for charge redistribution, the 4 highest similarity three-molecule alignments have been depicted in Figure 3. Note the close relationship between the I′ (top-left) and II′ (top-right) alignments and the III′ (bottom-left) and IV′ (bottom-right) alignments. While the NEVI conformer varies (NEVI(1) in I′ and IV′, and NEVI(2) in II′ and III′), the relative position between the conformationally adapted TIBO and αAPA structures is consistent in each pair of alignments (I′–II′ and III′–IV′). The best three-molecule alignment (I′, top-right in Figure 3) obtained from this ab initio similarity study is in excellent agreement with both the best three-molecule alignment obtained when

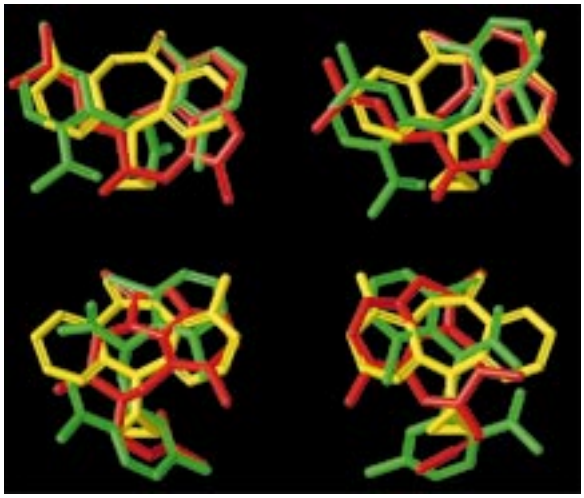

Figure 3. Best (top-left), second best (top-right), third best (bottom-left), and fourth best (bottom-right) conformationally flexible multi-molecule alignment solutions. NEVI, TIBO, and αAPA are colored in yellow, red, and green, respectively.

using the crystal structures of the inhibitors (RMS = 0.71 Å) and the experimental relative binding orientation of the inhibitors when forming a complex with the protein receptor (RMS = 0.94 Å) [31]. Therefore, although the ability of molecular-field-based similarity methods to assess the 'correct' relative binding orientation of molecules had been already validated on different sets of molecules in their bioactive conformation [30, 31], the present results elevate to a higher degree the use of this computational tool for obtaining quality hypothetical binding models at the initial stages of drug design processes, when crystal structures of effector molecules forming a complex with the protein receptor site are not available yet.

Conclusions

In summary, results obtained from conformationally rigid and conformationally flexible matching using pairwise similarities have revealed some significant issues. At the conformationally rigid level, the pairwise alignments in qualitative agreement with the 'experimental' alignment may not be ranked among the highest similarity indices. Further, as expected, optimization at the conformationally flexible level always increases the value of the similarity index but this does not necessarily mean improvement in the similarity ranking of the alignment in qualitative agreement with the 'experimental' alignment.

Interestingly, it also has been found that different alignment solutions obtained at the conformationally rigid level may eventually converge to the same alignment solution at the conformationally flexible level. This shows that by using a flexible-molecular similarity approach, a rational selection of a small diverse set of representative conformations for each molecule from a large number of conformations can be sufficient for assessing their relative alignment at the binding site in biological systems.

The importance of going beyond pairwise similarities has been also manifested in this study. Including conformational flexibility and charge redistribution in this molecular-field-based similarity study has resulted in the three-molecule alignment with largest similarity index to be in closest agreement with the 'experimental' alignment. Furthermore, individual conformationally adapted structures within this alignment were found to be in nearly as good or better agreement with their respective crystal structures than was found in the initial energy minimum structures.

However, it should be stressed that the results presented in this work also show that alignment solutions obtained from the use of flexible matching should always be used with caution. In an a priori study, one of the main uncertainties when using molecular-field-based similarity approaches to perform flexible matching is that the 'moving' fragments of one molecule may overlap with fragments of another molecule in a way that may not correspond to the binding conformation. This becomes a serious problem when molecules of significantly different sizes are treated, because the smaller molecules will always attempt to overlap optimally with the larger ones. However, this is an intrinsic caveat when using any similarity-based method.

Acknowledgements

We would like to thank Joe Moon and Jim Blinn for integrating MIMIC in the graphical user interface environment of the MOSAIC molecular modeling program.

References

1. Johnson, M.A. and Maggiora, G.M. (Eds.), Concepts and Applications of Molecular Similarity, Wiley, New York, NY, 1990.
2. Kubinyi, H. (Ed.), 3D QSAR in Drug Design: Theory, Methods and Applications, ESCOM, Leiden, 1993.
3. Dean, P.M. (Ed.), Molecular Similarity in Drug Design, Blackie Academic, London, 1995.
4. Martin, Y.C., J. Med. Chem., 35 (1992) 2145.
5. Lajiness, M., In van de Waterbeemd, H. (Ed.), Structure-Property Correlations in Drug Research, Landes Bioscience, Austin, TX, 1996, Chapter 5.
6. Lewis, R.A., Mason, J.S. and McLay, I.M., J. Chem. Inf. Comput. Sci., 37 (1997) 599.
7. Matter, H., J. Med. Chem., 40 (1997) 1219.
8. Mayer, D., Naylor, C.B., Motoc, I. and Marshall, G.R., J. Comput.-Aided Mol. Design, 1 (1987) 3.
9. Van Drie, J.H., Weininger, D. and Martin, Y.C., J. Comput.-Aided Mol. Design, 3 (1989) 225.
10. Martin, Y.C., Bures, M.G., Danaher, E.A., DeLazzer, J., Lico, I. and Pavlik, P.A., J. Comput.-Aided Mol. Design, 7 (1993) 83.
11. Willett, P., J. Mol. Recogn., 8 (1995) 290.
12. Pickett, S.D., Mason, J.S. and McLay, I.M., J. Chem. Inf. Comput. Sci., 36 (1996) 1214.
13. Van Drie, J.H., J. Comput.-Aided Mol. Design, 11 (1997) 39.
14. Klebe, G., In Kubinyi, H. (Ed.), 3D QSAR in Drug Design: Theory, Methods and Applications, ESCOM, Leiden, 1993, pp. 173–199.
15. Carbó, R., Leyda, L. and Arnau, M., Int. J. Quantum Chem., 17 (1980) 1185.
16. Hodgkin, E.E. and Richards, W.G., Int. J. Quantum Chem. Quantum Biol., 14 (1987) 105.
17. Petke, J.D., J. Comput. Chem., 14 (1993) 928.
18. Good, A.C., J. Mol. Graphics, 10 (1992) 114.
19. Kearsley, S.K. and Smith, G.M., Tetrahedron Comput. Methodol., 3 (1990) 615.
20. Hermann, R.B. and Herron, D.K., J. Comput.-Aided Mol. Design, 5 (1991) 511.
21. Sanz, F., Manaut, F., Rodríguez, J., Lozoya, E. and López-de-Briñas, E., J. Comput.-Aided Mol. Design, 7 (1993) 337.
22. Good, A.C., So, S.-S. and Richards, W.G., J. Med. Chem., 36 (1993) 433.
23. Perkins, T.D.J., Mills, J.E.J. and Dean, P.M., J. Comput.-Aided Mol. Design, 9 (1995) 479.
24. Jain, A.N., Dietterich, T.G., Lathrop, R.H., Chapman, D., Critchlow, Jr., R.E., Baner, B.E., Webster, T.A. and Lozano-Pérez, T., J. Comput.-Aided Mol. Design, 8 (1994) 635.
25. Grant, J.A., Gallardo, M.A. and Pickup, B.T., J. Comput. Chem., 17 (1996) 1653.
26. Klebe, G., Mietzner, T. and Weber, F., J. Comput.-Aided Mol. Design, 8 (1994) 751.
27. McMartin, C. and Bohacek, R.S., J. Comput.-Aided Mol. Design, 9 (1995) 237.
28. Lemmen, C. and Lengauer, T., J. Comput.-Aided Mol. Design, 11 (1997) 357.
29. Mestres, J., Rohrer, D.C. and Maggiora, G.M., J. Comput. Chem., 18 (1997) 934.
30. Mestres, J., Rohrer, D.C. and Maggiora, G.M., J. Mol. Graphics Mod., 15 (1997) 114.
31. Mestres, J., Rohrer, D.C. and Maggiora, G.M., J. Comput.-Aided Mol. Design, 13 (1999) 79.
32. Klebe, G., Perspect. Drug Discov. Design, 3 (1996) 85.
33. Leach, A.R., In Dean, P.M. (Ed.), Molecular Similarity in Drug Design, Blackie Academic, London, 1995, pp. 57–88.
34. Marshall, G.R., Barry, C.D., Bosshard, H.E., Dammkoehler, R.A. and Dunn, D.A., In Olson, E.C. and Christoffersen, R.E. (Eds.), Computer-Assisted Drug Design, ACS Symposium Se-

ries, No. 112, American Chemical Society, Washington, DC, 1979, pp. 205–222.
35. Perkins, T.D.J. and Dean, P.M., J. Comput.-Aided Mol. Design, 7 (1993) 155.
36. Allinger, N.L., J. Am. Chem. Soc., 99 (1977) 8127.
37. Mohamadi, F., Richards, N.G.J., Guida, W.C., Liskamp, R., Lipton, M., Caufield, C., Chang, G., Hendrickson, T. and Still, W.C., J. Comput. Chem., 11 (1990) 440.
38. Goodman, J. and Still, W.C., J. Comput. Chem., 12 (1991) 1110.
39. Rohrer, D.C., In Carbó, R. (Ed.), Molecular Similarity and Reactivity: From Quantum Chemical to Phenomenological Approaches, Kluwer Academic Publishers, Dordrecht, 1995, pp. 141–161.
40. Dewar, M.J.S., Zoebisch, E.G., Healy, E.F. and Stewart, J.J.P., J. Am. Chem. Soc., 107 (1985) 3902.
41. Good, A.C., Hodgkin, E.E. and Richards, W.G., J. Chem. Inf. Comput. Sci., 32 (1992) 188.
42. Merluzzi, V.J., Hargrave, K.D., Labadia, M., Grozinger, K., Skoog, M., Wu, J.C., Shih, C.-K., Eckner, K., Hattox, S., Adams, J., Rosenthal, A.S., Faanes, R., Eckner, R.J., Koup, R.A. and Sullivan, J.L., Science, 250 (1990) 1411.
43. Kukla, M.J., Breslin, H.J., Pauwels, R., Fedde, C.L., Miranda, M., Scott, M.K., Sherrill, R.G., Raeymaekers, A., Van Gelder, J., Andries, K., Janssen, M.A.C., De Clercq, E. and Janssen, P.A.J., J. Med. Chem., 34 (1991) 746.
44. Pauwels, R., Andries, K., Debyser, Z., Van Daele, P., Schols, D., Stoffels, P., De Vreese, K., Woestenborghs, R., Vandamme, A.-M., Janssen, C.G.M., Anne, J., Cauwenbergh, G., Desmyter, J., Heykants, J., Janssen, M.A.C., De Clercq, E. and Janssen, P.A.J., Proc. Natl. Acad. Sci. USA, 90 (1993) 1711.
45. Bernstein, F.C., Koetzle, T.F., Williams, G.J.B., Meyer Jr., E.F., Brice, M.D., Rodgers, J.R., Kennard, O., Shimanouchi, T. and Tasumi, M., J. Mol. Biol., 112 (1977) 535.
46. Kohlstaedt, L.A., Wang, J., Friedman, J.M., Rice, P.A. and Steitz, T.A., Science, 256 (1992) 1783.
47. Ding, J., Das, K., Tantillo, C., Zhang, W., Clark Jr., A.D., Jessen, S., Lu, X., Hsiou, Y., Jacobo-Molina, A., Andries, K., Pauwels, R., Moereels, H., Koymans, L., Janssen, P.A.J., Smith Jr., R.H., Koepke, M.K., Michejda, C.J., Hughes, S.H. and Arnold, E., Structure, 3 (1995) 365.
48. Ding, J., Kalysn, D., Moereels, H., Koymans, L., Andries, K., Janssen, P.A.J., Hughes, S.H. and Arnold, E., Nat. Struct. Biol., 2 (1995) 407.